Lasers in Manufacturing Conference 2019

Cutting of composite materials: a quality and processing time optimized scan strategy for GFRP and CFRP

Frank Schneider[a*], Dirk Petring[a], Norbert Wolf[a]

[a] *Fraunhofer Institute for Laser Technology, Steinbachstr. 15, 52074 Aachen, Germany*

Abstract

Glass fiber and carbon fiber reinforced plastics (GFRP, CFRP) play an important role in the material mix of automotive and aerospace components. Light weight design has to be consistent with the availability of an efficient production technology. Cutting of these materials with multi kW-fiber lasers enables the demanded cutting speeds in the range of meters per minute. An optimization procedure is presented for a multi-pass process in order to achieve high quality cut edges and short processing times by appropriate setting of scan speed and interval times between scans. The process is demonstrated by trimming a car roof bow. Following a multi material approach, the part consists of two stacked layers of GFRP and CFRP at the cut path. Since the length of the cut is 800 mm at each side of the roof bow, the scan field (200x200 mm²) is moved continuously over the workpiece, demonstrating the applicability for bigger components.

Keywords: CFRP cutting, GFRP cutting, fiber laser cutting, multi-pass, scan strategy

1. Introduction

High edge quality with narrow heat affected zones (HAZs) and profitable cutting speeds are primary requirements on laser cutting processes of composite material. While short and ultra short pulsed lasers allow high edge quality in laser cutting with HAZs < 20 µm as shown in C. Freitag et al 2015, multi-kilowatt high power cw lasers offer high cutting rates of several meters per minute at acceptable quality with a HAZ in a range of 50-100 µm in optimized processes (J. Stock 2017, R. Staehr et al. 2016). To achieve this, a multi-pass scanning technique with fast beam deflecting devices is used to dissipate the heat input into small portions. Scan speed and the interval time between one scan and the next are parameters to control the heating of the kerf bottom

* Corresponding author. Tel.: +49-241-8906-426; fax: +49-241-8906-121 .
E-mail address: frank.schneider@ilt.fraunhofer.de .

and walls by the laser beam.

At low scan speed the long laser-material interaction time and a high volume of ablated material lead to a high thermal load. Accordingly, the heat impact caused by a single scan can be reduced by increasing the scan speed at the expense of the amount of removed material. Typically the following scan is carried out before the initial temperature of the material is reached again. Consequently the temperature level rises from scan to scan and this heat accumulation can cause thermal damage that increases with shorter scan to scan interval times. For pulsed processes this scenario has to be expanded by considering also the influence of heat input by single pulses and by pulse overlap, as it is systematically and detailed explained by R. Weber et al, 2017.

The multi-pass processing is applied in particular to carbon fiber reinforced material. If glass fiber material is cut with a laser, typically a single pass gas supported standard process is used, because in contrast to carbon the glass is predominantly transformed into the molten phase during cutting and thus the process profits from a gas supported ejection. In addition, glass fibers have a lower heat conductivity and many glass composites consist of randomly oriented fibers. Both diminish the dispersion of a large HAZ. Because of the high absorption in glass, CO_2-lasers are the preferred laser source for glass composites. If the matrix material is filled with absorbing additives like carbon black, also 1 µm beam sources can be used (F. Schneider et al, 2015). However, in the study presented here also GFRP is cut in a multi-pass scanning process without cutting gas, because a demonstrator part made from sandwich material with a layer of CFRP and GFRP should be processed in one processing step.

2. Mixed material demonstrator

The demonstrator consisting of this material mix is a hybrid car roof bow (Fig. 1). The requirements and dimensions of the part are based on an original CFRP-part from the BMW 7 series. The new design utilizes a GFRP and CFRP material mix. The base material is a compression mold glass fiber PA6 composite with 40 vol% randomly oriented fibers. At the ends of the part a metal plate is joined to the composites during the molding process. This joint reaches its strength without adhesives thanks to a pretreatment by laser micro-structuring of the metal surface leading to a mechanical interlocking between the two materials (D. Spancken et al. 2018). The GFRP is reinforced with unidirectional (UD) carbon fiber tapes in the longitudinal direction of the roof bow. At the long edges the part has to be trimmed to its final dimension, requiring a cut through CFRP in the top half of the material and GFRP in the bottom half, each 1.2 mm in thickness.

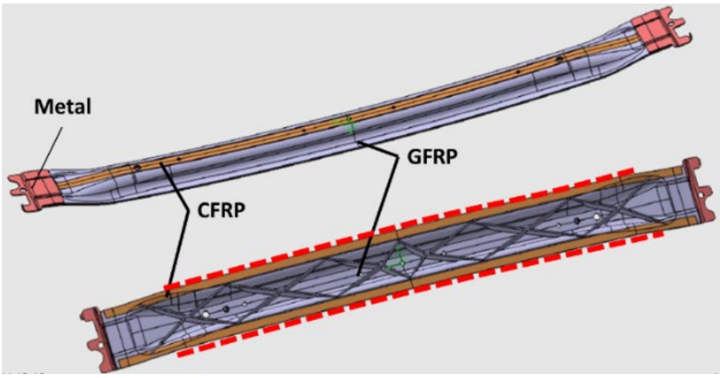

Fig.1. Car roof bow demonstrator after trimming to final dimension. Red lines mark the cut path on both sides of the part. CFRP stiffeners are colored brown, the GFRP body part is colored grey and the metal plates at both end in light red.

3. Experimental procedure and cutting setup

The edge trimming is performed with a 5 kW single mode fiber laser (IPG YLS-5000) and a prototype galvo-Scanner from SCANLAB in a multi-pass process. The measured focus diameter is 50 µm, resulting from imaging the fiber with 30 µm diameter with a collimation unit, focal length 200 mm, a scanner internal beam expansion with a factor 1.38 and a F-theta optics with 420 mm focal length. The maximum scan speed is 35 m/s. Process emissions are blown to the scrap side of the cut by a transversal crossjet (air). This setup, using high scan speeds and high intensity, is in particular suitable for cutting CFRP, but since the stacked material of the demonstrator should be cut in one process step, it is also used for cutting the GFRP layer.

The scan speed and the interval time between two scans are the varied parameters to find the dependence on cut edge quality and total processing time. The interval time is defined as the time between processing a place of the cut path and processing the same place in the subsequent scan the next time. The direction of the processing is the same for each scan. For all cuts the laser power is 5 kW.

To acquire the course of temperature on the surface and in the kerf between the scans, an IR-camera is used, targeted on the process in top view at an angle of 45° and aligned to the cut direction. The thermal videos yield a resolution of 77 µm/pixel and 200 Hz frame rate.

4. Results and discussion

The number of required scans for a complete separation increases linear with the scan speed, as shown in **Fig. 2**. Avoiding a dominant scan to scan heat accumulation by sufficient interval time between the scans, the edge quality improves with increasing scan speed. Low scan speed increases the HAZ and leads to an irregular flank geometry with uncontrolled protruded fibers. In Fig. 3a this is demonstrated with the extreme example of a scan speed of 0.3 m/s resulting in a complete separation in one pass. The heating of the edge softens the matrix material and forced by the evaporation pressure fibers are excavated from the matrix. This is notably facilitated by the cut direction being parallel to the fiber direction. In contrast to material with multiaxial layup, with UD material long fiber bundles along the cut flank are located in the softened zone and can be completely or partly excavated. At 2 m/s scan speed still edge delamination of the carbon fiber layer is visible (Fig. 3b).

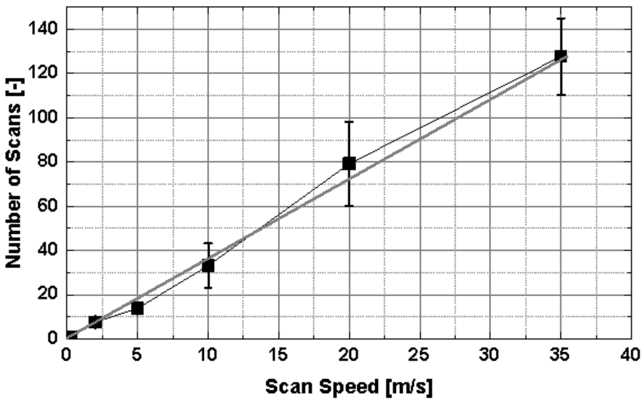

Fig.2. Number of required scans for complete separation.

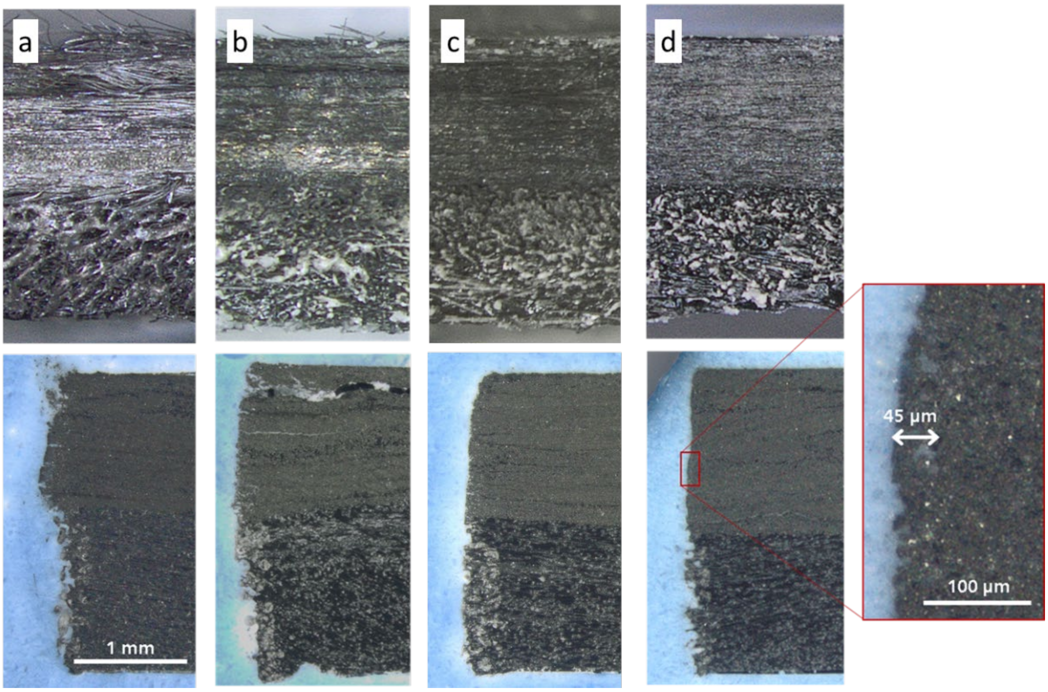

Fig.3. Cut edge (top) and cross sections of cuts (bottom) with (a) scan speed 0.3 m/s (1 scan); (b) 2m/s (7 scans,); (c) 5m/s (15 scans) and; (d) 10 m/s (24 scans), 500 ms interval time.

The speeds at and above 5 m/s give the best results with a high flank accuracy, marginal protruding fibers and a small HAZ. The HAZ is hardly identifiable in comparison with the anyway existing irregularities of the base material. Even with most critical inspection the HAZ is below 50 µm.

The thermal impact from a single scan is overlaid by scan to scan heat accumulation. Fig. 4 shows the temperature measurement of the kerf over time for two interval times, averaged over a 20 mm long evaluation line positioned in the middle of the kerf. Each scan generates a peak, followed by a cooling period due to heat conduction into the surrounding material and convective heat transport by the cross jet flow. The short interval time of 150 ms causes a rapid temperature increase even for the minimum temperature at the end of the cooling time. Compared to the longer interval time of 550 ms, the total summed up time over all passes that a critical temperature is exceeded is by a factor of 3 longer, if the melting temperature 215° C is seen as critical. Corresponding to the progress of the kerf-bottom temperature, the HAZ in the CFRP layer with the short interval time is 400 µm, whereas it is reduced to 50 µm, when the long interval time is applied.

The change from the CFRP to GFRP processing comes along with a stronger heat accumulation. In Fig. 4 this can be seen in the discontinuity of the slope of the orange line that marks the envelope of the minimum temperature after each pass. This can be explained by residue particles of molten glass that remain in the kerf, visible on the cut edge in Fig.3, and by the generally different material properties.

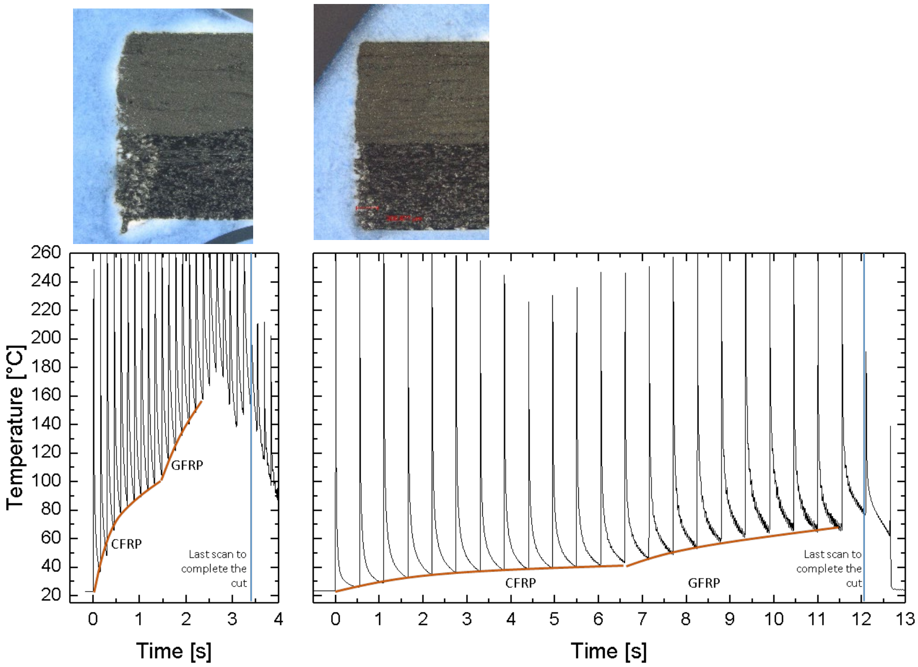

Fig.4. Temperature in the kerf vs. time and corresponding cross sections of the flanks for an interval time of 150 ms (left) and 550 ms (right) at a scan speed of 10 m/s.

The heat propagation from the kerf into the adjacent material at the surface is shown in Fig. 5. The thermal videos are processed to streak images. The temperature is measured on an evaluation line of 2.6 mm length perpendicular to the cut for each frame of the video and displayed over time with 5 ms resolution. Frames during the processing had to be discarded, because hot vapor and emitted particles disturb the thermal image (white lines in Fig. 5). The streak images show that for short interval times high temperatures in the kerf and in the zone adjacent to kerf persist longer after a pass than for long interval times.

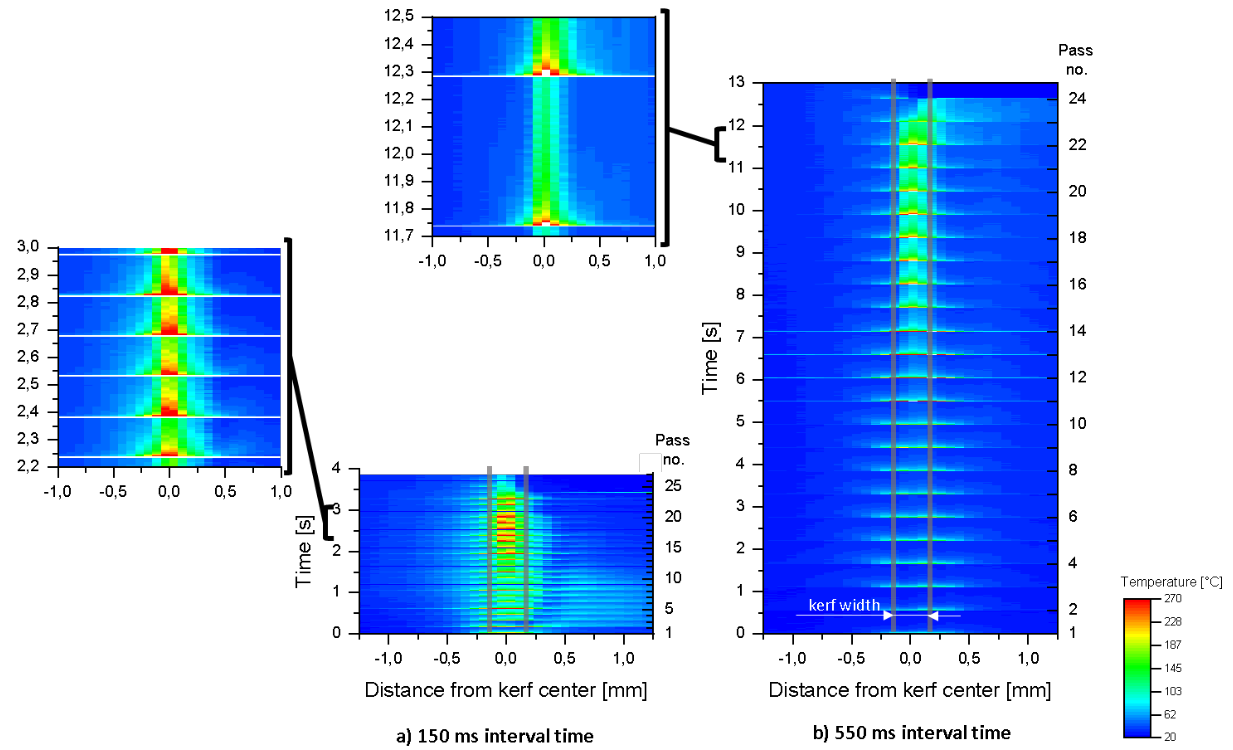

Fig.5. Temperature field perpendicular to the cut path over time for two interval times a) 150 ms and b) 550 ms (scan speed 10 m/s), showing the higher temperature load of the edges at short interval times. The enlargements shortly before the end of the cut show, that after each pass high temperatures in the kerf are hold for a longer time with short interval time. The white lines are video frames during the processing, which cannot be evaluated due to oversteer and image falsification by hot vapor emissions.

The kerf width at the surface is in the range of 300 µm to 450 µm, depending on the parameters, and is increasing with the processing depth. With this kerf width it can be estimated that the lower kerf and bottom of the kerf is visible in the thermal videos in two central lines of pixels, the upper kerf and the kerf edges in one or two further lines of pixels on each side of this central zone. More outside of these center lines the surface is visible. A resolution of 77 µm and shadowing effects with increasing processing depth do not allow a more spatially detailed interpretation. With this classification into zones the temperature field in the streak images shows that the most significant heat impact results from the hot remaining material at the kerf bottom.

A kerf width between 300 µm and 400 µm is a factor of 3-5 wider than the laser spot size at the surface. A plausible explanation are secondary material removal mechanisms, induced by hot vapor emissions and scattered laser radiation, forming a secondary heat source. This effect is significantly more pronounced for unidirectional material that is cut in fiber direction than perpendicular to the fiber direction, as it is shown for the hybrid material in two cross sections in Fig. 6, left. Two reasons explain this difference:

First, the heat conduction of the fibers is a factor of five to ten higher in fiber direction than perpendicular to the fibers. This promotes a heat accumulation at the edge for parallel fibers and a higher heat dissipation into the material for perpendicular fibers.

Second, in parallel cuts long fiber segments can easily be separated from the matrix, whereas in cuts perpendicular to the fibers the cold matrix more far away from the edge keeps the fibers in the compound.

In the latter case the fiber and matrix material is not removed from the edge, but the matrix material shows a wider heat effected zone than in parallel cuts. For multiaxial material this effect can be seen from layer to layer with an alternating ablation width as exemplarily shown in Fig. 6, right.

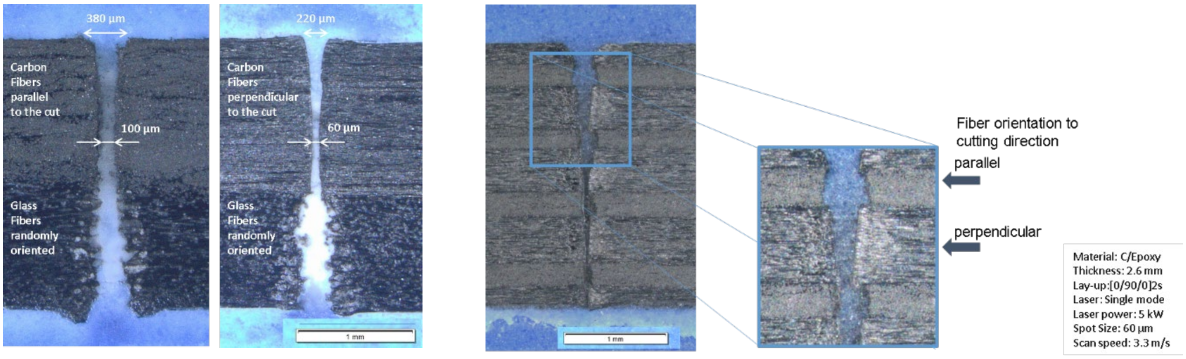

Fig.6. Dependence of the kerf width on the fiber orientation for the hybrid demonstrator material (left cross sections) and alternating ablation characteristic for a multiaxial CFRP (right cross section).

To achieve high quality cut edges, the scan speed should be chosen high, requiring a high number of passes, and the interval time should be long. Both leads to long total processing times, because the total processing time t_{total} is given by

$$t_{total} = n_{req} * t_{int} \tag{1}$$

with n_{req} the number of passes needed for the cut and t_{int} the interval time between two passes. Assuming that the same path is processed in the same direction in every pass, n_{req} and t_{int} can be written as

$$n_{req} = c\, v_{scan} \tag{2}$$

$$t_{int} = t_{process} + t_{pos} + t_{idle} = \frac{l_{scan}}{v_{scan}} + t_{loss} \tag{3}$$

where $t_{process}$ is the time for scanning the path of length l_{scan} with the laser at the scanning speed v_{scan}, t_{pos} the time for positioning to the starting point of the path, t_{idle} the waiting time before starting the next pass and c a constant considering material and processing parameters (kind of material and thickness, laser power, focusing conditions, cross jet influence). t_{pos} and t_{idle} are summed up to the loss time t_{loss}. With (2) and (3) the total processing time t_{total} is

$$t_{total} = c(l_{scan} + v_{scan} t_{loss}) \tag{4}$$

For a required total processing time t_{total} the product of the scan speed v_{scan} and the time t_{loss} allows various combinations of v_{scan} and t_{loss}, limited just by technical constraints as the maximum possible scan speed and acceleration. However, these parameter combinations of the scan speed and the time t_{loss} define the achievable HAZ of the cut edge.

In Fig. 7 this is separately shown for the CFRP and GFRP layer of the demonstrator material. The HAZ is presented in dependence of the scan speed v_{scan} for three total processing times. By this also the time t_{loss} for each scan speed and total processing time t_{total} is defined and shown as a color mark for each point.

For the CFRP layer the curves have a minimum HAZ, giving the best scan speed and time t_{loss} for a specific total processing time. The mininum HAZ is lower for high total processing times, allowing both high scan speeds paired with a sufficient time t_{loss}. To the left of the minima the HAZ increases, because material degradation occurs caused by the low scan speed. To the right of the minima the HAZ increases, because the interval times are decreasing and heat accumulation from scan to scan prevents a better quality.

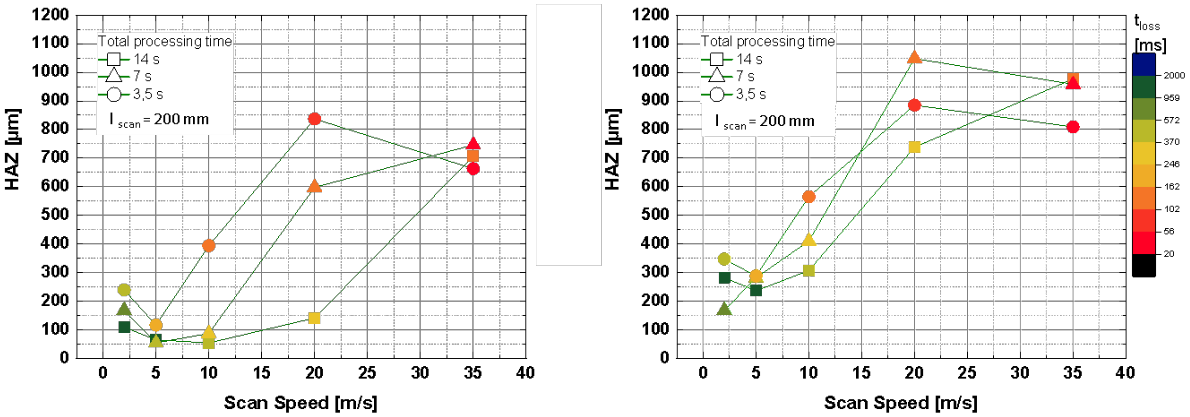

Fig.7. HAZ vs scan speed for three total processing times t_{total}. With the scan speed and the total processing time also the interval times t_{int} and the lost times t_{loss} are defined (color scale). The HAZ is separately evaluated for the CFRP (left) and GFRP (right) layer of the hybrid material.

5. Demonstrator processing

According to Fig. 7, a scan speed of 5 m/s and an interval time of 250 ms was chosen as a good trade-off between quality and productivity, considering both sandwich materials, CFRP and GFRP.

The cut path is a straight line on both sides of the demonstrator with 800 mm length and oriented parallel to the UD-carbon fiber orientation. Because the length of the cut path exceeds the size of the scan field (200x200 mm²), a robot moves the scan field over the demonstrator part to cover the whole length. Because the lightweight part (final weight 0.5 kg) is easier to handle than the scanner, the workpiece is moved under the stationary scanner. During the continuous movement of the robot the scanner processes with its superposed axis for the fast beam movement repeatedly a section of the cut path in the scan field (Fig. 8).

With the chosen scan speed and interval time the resulting proceeding speed of the scan field is defined such that the number of required scans is reached, when the entire scan field has passed by. The corresponding speed for the relative movement between the workpiece and the scan field is 50 mm/s.

Requiring 60 ms for the processing and the positioning in one scan, from the interval time of 250 ms remains an unproductive idle time of 190 ms. This time can efficiently be used to process the second side of the demonstrator in the same operation.

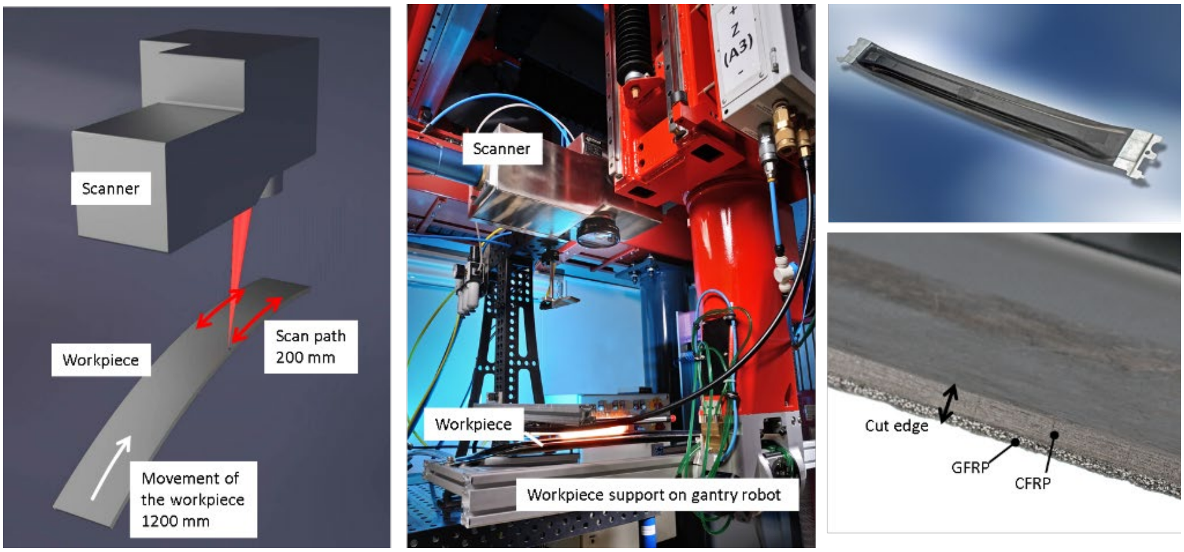

Fig.8. Arrangement of scanner and workpiece movement (left), processing of the demonstrator on a gantry robot (middle) and finished demonstrator with a detail showing the cut edge (right).

6. Conclusion

Even though fast scan speed and long interval times between scans enable a small HAZ in multi pass cutting, the smallest HAZ within a limited, predefined processing time is achieved when an optimal pairing of scan speed and interval time is used. This matching balances between a high scan speed to prevent unnecessary heat load per scan and a low scan speed, leading to a corresponding low number of required passes, to reduce heat accumulation from scan to scan to a minimum.

Applied to trimming of a car roof bow demonstrator part of CFRP and GFRP hybrid material, the optimization yields high quality cut edges and meets the demands on acceptable processing times. To allow a smooth processing of the trim path of 800 mm length on each side of the roof bow, the scan field is continuously moved while the cut kerf is successively formed with the fast scanning multi pass process, demonstrating that the multi pass process is applicable also for big contours without stitching.

Acknowledgement

This work was funded by the German Federal Ministry of Education and Research BMBF in the frame of the project HyBriLight under grant number 13N12718.

References

C. Freitag, M. Wiedenmann, J.-P. Negel, A. Loescher, V. Onuseit, R. Weber, M. Abdou Ahmed, T. Graf: High-quality processing of CFRP with a 1.1-kW picosecond laser, Appl. Phys., A Mater. Sci. Process. 119(4), 1237–1243 (2015).

F. Schneider, N. Wolf, C. Engelmann, W. Moll, D. Petring: Laser Cutting and Joining in a Novel Process Chain for Fibre Reinforced Plastics, LIM 2015, 8th International WLT-Conference on Lasers in Manufacturing, Proceedings, München, DE, Jun 22-25, 2015.

D. Spancken, K. van der Straeten, J. Beck et al.: Laser Structuring of Metal Surfaces for Hybrid Joints, Lightweight Design worldwide, Volume 11, Issue 4, pp 16–21, 2018, https://doi.org/10.1007/s41777-018-0028-6.

R. Staehr, S. Bluemel, P. Jaeschke, O. Suttmann, L. Overmeyer: Laser cutting of composites—Two approaches toward an industrial establishment, Journal of Laser Applications 28, 2016.

J.Stock, Remote-Laserstrahltrennen von kohlenstofffaserverstärktem Kunststoff, Diss., München, Techn. Univ., 2017, S. 112.

R. Weber, T. Graf, C. Freitag, A. Feuer, T. Kononenko, V. Konov: Processing constraints resulting from heat accumulation during pulsed and repetitive laser materials processing, Opt. Express 25, 3966-3979, 2017.